

Single Molecule Nanometronome

Chittanon Buranachai,[†] Sean A. McKinney,[‡] and Taekjip Ha^{*,†,‡,§}

Center for Biophysics and Computational Biology and Department of Physics,
University of Illinois at Urbana-Champaign and Howard Hughes Medical Institute,
Urbana, Illinois 61801

Received December 18, 2005; Revised Manuscript Received January 30, 2006

ABSTRACT

We constructed a DNA-based nanomechanical device called the nanometronome. Our device is made by introducing complementary single-stranded overhangs at the two arms of the DNA four-way junction. The ticking rates of this stochastic metronome depend on ion concentrations and can be changed by a set of DNA-based switches to deactivate/reactivate the sticky end. Since the device displays clearly distinguishable responses even with a single base pair difference, it may lead to a single molecule sensor of minute sequence differences of a target DNA.

DNA-based nanomachines and nanodevices have increased rapidly in popularity in recent years.^{1–4} The variety of their forms originates from careful control of molecular recognition between nucleotides, and their functions are based on changes between possible conformations. These conformational changes are in general effected by changes in solution conditions, such as ionic strength,^{5,6} pH,^{7,8} or temperature,⁹ or by applying short “fuel” oligonucleotides that selectively interact with a specific part of the device.^{10,11} Here we introduce a DNA-based nanodevice that undergoes thermally driven structural changes whose switching rate is user controllable. We call our device the “single molecule nanometronome” because the “ticking” rates measured from individual nanodevices can be manipulated by magnesium ion concentration and by addition of partially complementary DNA strands.

The nanometronome can be viewed as the marriage between a “molecular beacon”^{12,13} and the four-way DNA Holliday junction.¹⁴ It is composed of four single-stranded DNA forming a four-way junction with two extra single-stranded overhangs capable of forming base pairs with each other (Figure 1A). In the presence of divalent metal ions such as Mg²⁺ ($\geq 100 \mu\text{M}$),¹⁵ the Holliday junction folds into compact conformations called stacked-X structures.¹⁶ There are two stacked-X conformers (Figure 1A; *IsoI*, helix H stacks on helix B/helix R stacks on helix X; and *IsoII*, helix B stacks on helix X/helix H stacks on helix R) and single molecule measurements have shown that the two conformers are in continual exchange on the millisecond time scale.^{17,18} The DNA sequence at the strand exchange point dictates how one conformer is preferred over the other¹⁵ and the rates of transition between them strongly depend on the type and

concentration of metal ions in solution.^{17,18} In order for the conformational transitions to occur between the two compact conformers, it is thought that the molecule must go through an intermediate open structure (structure 2 in Figure 1A), which becomes highly populated in the absence of metal ions. However, the open structure cannot be directly resolved in magnesium solution even in single molecule measurements, possibly as a result of limited time resolution.^{17,18}

Here, we chose a junction sequence (called junction 7) without any significant conformational bias,^{17,19} that is, the lifetimes of the two conformers are similar before imposing external conformational constraints. The addition of two single-stranded overhangs at the end of two helical arms (helixes B and H, Figure 1) introduces an extra conformer (structure 4), which is similar to structure 3 but stabilized due to the base pairing of the sticky ends. This extra conformer, likely to have the same global junction conformation (*IsoII*), would force the nanometronome to preferentially stay in one conformation (*IsoII*) over the other (*IsoI*), hence altering the ticking rates of the nanometronome. The sequence information of the junction and the overhangs can be found in Figure S1, Supporting Information.

Real time structural changes of the nanometronome are monitored at the single molecule level via Förster resonance energy transfer (FRET) using a total internal reflection fluorescence microscope. The donor (Cy3) and acceptor (Cy5) are attached to the ends of helix H and helix B, respectively (Figure 1). As the efficiency of FRET, E , scales as a reciprocal of the sixth power of donor–acceptor intermolecular distance R , $E = 1/(1 + (R/R_0)^6)$,²⁰ upon exciting the donor with a 532 nm laser, the low FRET state (stronger donor emission) corresponds to the junction in *IsoI* (structure 1) in which two fluorophores are substantially separated whereas the high FRET states (stronger acceptor emission) represent the junction in *IsoII* (and nanometronome

* To whom correspondence may be addressed. E-mail: tjha@uiuc.edu.

[†] Center for Biophysics and Computational Biology, University of Illinois.

[‡] Department of Physics, University of Illinois.

[§] Howard Hughes Medical Institute.

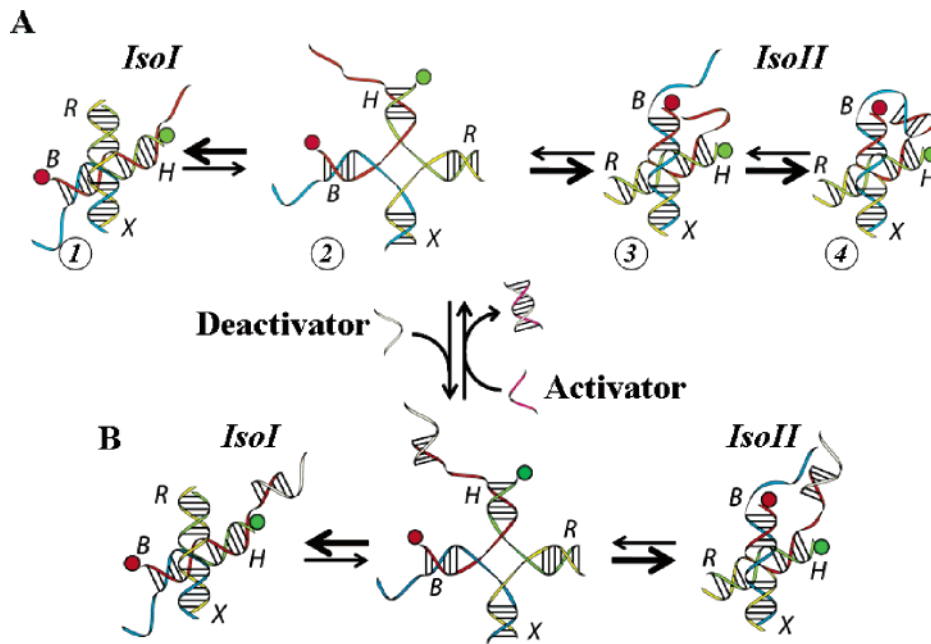


Figure 1. (A) Diagram of conformational changes of a nanometronome. In terms of native four-way Holliday junctions, structure 1 possesses conformation *IsoI* whereas structure 3 and structure 4 possess conformation *IsoII*. Structure 2 is believed to be a transition or intermediate state during transitions. Base pairing of the sticky ends lowers the free energy of the structure 4 forcing the nanometronome to stay in conformation *IsoII* longer. The presence of Mg^{2+} is critical for the transitions to occur, and the rates of transition depend on $[Mg^{2+}]$ (see text). (B) Reversibly switching sticky ends on and off by utilizing the short single-stranded deactivator/activator. The deactivator competitively binds onto the single-stranded overhang at the end of helix H, silencing the sticky ends. This binding leaves an overhang handle for the activator to bind and later remove the deactivator via three-stranded branch migration.

in either structure 3 or structure 4). The single molecule FRET efficiency, E , is approximated by the acceptor intensity divided by the sum of the donor and acceptor intensities.

The presence of the partially complementary overhangs clearly biases the nanometronomes toward *IsoII* conformer (high FRET), as can be seen from the single molecule FRET time traces of the constructs with four base pair (bp) and five bp sticky ends (Figure 2A, top two traces). Even with just a single additional A–T basepair, the bias is significantly enhanced with the five bp sticky end compared to the four bp. Constructs with six bp and seven bp sticky ends increased the dwell times in the high FRET state even more so that most molecules stayed only in the high FRET state before undergoing photobleaching, precluding detailed analysis (data not shown).

To evaluate the homogeneity of many single molecules of nominally identical metronomes, we made a scatter plot of the average dwell times of the high FRET state vs the low FRET state in the logarithmic scale (Figure 2B). Each data point in the scatter plot represents a single nanometronome. The data from nanometronomes with four bp sticky end (red dots, 234 molecules) and with five bp sticky end (blue dots, 241 molecules) form distinct clusters, showing that heterogeneity between molecules, either statistical or intrinsic, is small enough to reveal reliably even one base pair difference in the single-stranded overhang. The clusters are much more clearly separated along the high FRET state axis than in the low FRET state axis, suggesting that the sticky end plays a much more significant role for *IsoII* as predicted. The low FRET state's average dwell times fall into the same range of that of unconstrained junction $7^{17,18}$

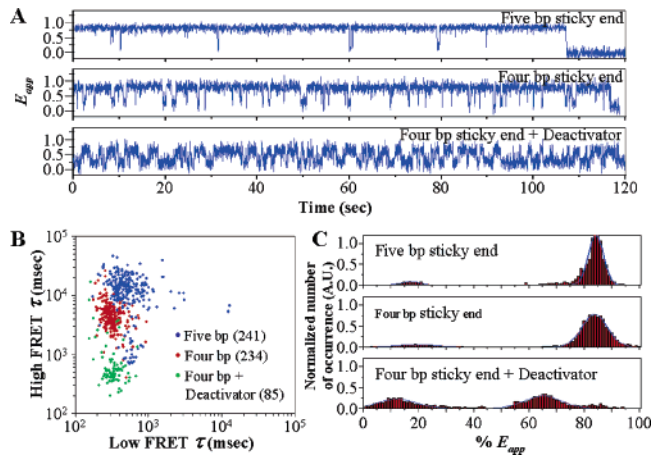


Figure 2. (A) Sample FRET traces from nanometronomes with five bp sticky end (top trace) four bp sticky end (middle trace) and silenced sticky end (bottom trace). The low FRET state corresponds to conformer *IsoI* and the high FRET state corresponds to the conformer *IsoII*. (B) A log–log plot of average high FRET (y axis) and low FRET (x axis) dwell times from the three groups of nanometronomes. Each spot represents a single nanometronome, and the numbers in parentheses in the figure legend indicate number of spots. (C) Normalized histogram plots of the apparent FRET efficiency ($E_{app} = I_A / (I_A + I_D)$). The increase in FRET efficiencies of the high FRET state caused by the sticky ends (from $E_{app} \approx 0.65$ in the case of silenced sticky end to $E_{app} \approx 0.83$ in the case of four bp and five bp sticky ends) indicates that the sticky ends bring two helical arms closer.

indicating that the presence of sticky ends does not drastically affect the dwell time of the *IsoI*.

Figure 2C (top and middle panels) shows that the FRET efficiency of the high and low FRET states is essentially

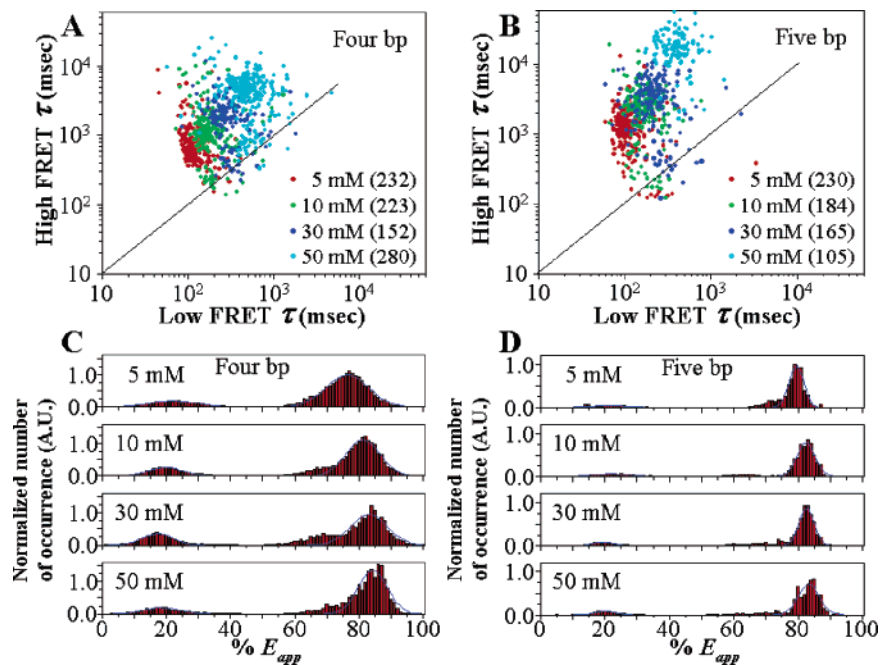


Figure 3. Dependence of the high FRET and low FRET average dwell times on $[Mg^{2+}]$ for nanometronomes with a four bp sticky end (A) and with a five bp sticky end (B). The numbers in parentheses indicate number of spots, and the solid line marks a 1:1 ratio of the two native dwell times (found in junction 7 without sticky ends). Larger deviation from the solid line suggests that Mg^{2+} might have a stronger effect on stabilizing the five bp sticky end. The increase in Mg^{2+} concentration correlates with the increase in the FRET values (C and D). There are two possible explanations for this behavior, one involves the junction itself and the other involves the sticky end (see text for more details).

identical for four bp and five bp sticky ends, $E \sim 0.85$. Whether this is because there is no distance difference or because FRET is not very sensitive to small distance differences in this range is not clear.

Next, we studied the effect of Mg^{2+} concentration on the nanometronome dynamics. Transition rates between two conformers of the Holliday junction depend strongly on the ionic strength. It has been shown¹⁷ that, over a range of sub-millimolar to several hundred millimolar in concentration,¹⁷ Mg^{2+} increases the dwell times of both conformers by screening the electrostatic repulsion between the phosphate backbones at the strand exchange point, thereby stabilizing the stacked conformations. Parts A and B of Figure 3 show that, for the nanometronomes too, the dwell times of both the high FRET state and the low FRET state increase as the concentration of Mg^{2+} is raised (Mg^{2+} concentration = 5, 10, 30, and 50 mM). The deviation from the solid reference line, which represents where the data from normal junction 7 is located (a 1:1 ratio of high FRET and low FRET dwell time), is due to the selective stabilization of the high FRET state by the sticky end. Not surprisingly, at the same salt concentration, the five bp sticky end (Figure 3B) yields a larger deviation from the reference line than the four bp sticky end (Figure 3A).

The increase in Mg^{2+} concentration also slightly raises the FRET efficiency of the high FRET state in both cases (Figure 3C,D). We discovered that in the case of junction 7, the high FRET peak values were also raised by the increasing Mg^{2+} concentration (data not shown) possibly due to a stronger screening of the high salt concentration at the strand exchange point resulting in the closer distance between the

FRET pairs. This may be what is happening in the case of the nanometronome as well. Another possible reason here is that Mg^{2+} also enhances the stability of the base pairing at the sticky end, making structure 4 relatively more populated than structure 3. It has been shown that a five bp sticky end (5' CCCAA- -TTGGG 3') within a molecular beacon undergoes sub-millisecond zipping–unzipping transitions and the equilibrium shifts to the zipped state with increasing salt concentration.¹³ If this is applicable to our case, the apparent FRET efficiencies we obtain may be a result of time averaging over multiple transitions between structure 3 and structure 4 within our time resolution (30 ms); the longer the nanometronome stays in structure 4 at higher Mg^{2+} concentrations, the higher the measured apparent FRET efficiencies. Another interesting observation is that Mg^{2+} stabilized the five bp sticky end more strongly than it did for the four bp sticky end, as can be seen from the higher slope in the scatter plot (Figure 3A,B).

Next, we introduce a mechanism to change the ticking rates of our nanometronome. The idea, as applied to various types of DNA-based nanoscaffolds^{10,11} and nanomachines,^{1,2,21} is based on two different, but fully complementary, short single-stranded DNA we call the deactivator and activator. The deactivator is capable of forming stable base pairing with the single-stranded overhang at the end of helix H. This deactivator binding silences the sticky end, turning the nanometronome into a normal junction 7 (Figure 1B). The reaction can be reversed by applying the activator. After the binding of the activator to the exposed region of the deactivator, a triple-stranded branch migration occurs, and eventually the deactivator leaves the sticky end because of

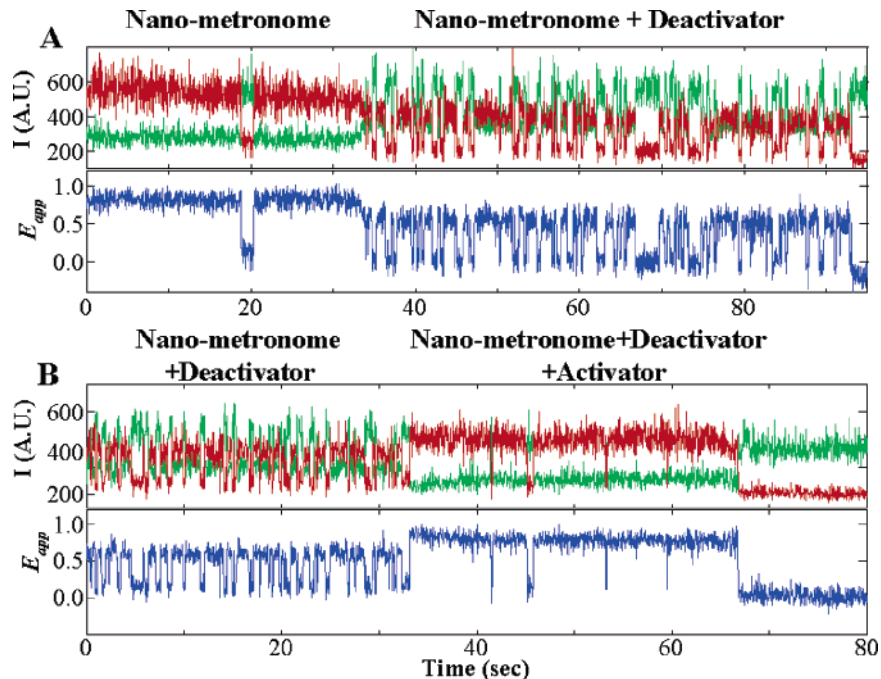


Figure 4. Monitoring the sticky ends being deactivated (A) and reactivated (B) in real time using a flow delivery system. Because of the slow rate of hybridization, high concentrations ($\sim 1 \mu\text{M}$) of both the deactivator and the activator are used to induce the transitions.

the formation of full duplex DNA between the activator and the deactivator which is energetically more stable. Afterward, the nanometronome returns to the original state (Figure 1A).

A sample trace from a silenced nanometronome (Figure 2A, bottom trace) clearly exhibits the much higher transition rates between the high FRET and low FRET states compared with those from nanometronomes with five bp and four bp sticky ends. Figure 2B compares the high FRET and low FRET dwell times of the nanometronomes (four bp version) with deactivated sticky ends (green dots, 85 molecules) to the nanometronomes having active four bp (red dots) and five bp (blue dots) sticky ends. The silenced sticky end yields an approximate 1:1 high FRET and low FRET dwell time as expected from a normal junction 7. The single molecule FRET histogram for the deactivated nanometronome (four bp version) (Figure 2C, the bottom plot) shows two peaks with comparable populations. The FRET value of the high FRET state ($E \sim 0.65$) is lower than that of four bp and five bp sticky ends and is similar to what was reported from junction 7 previously.¹⁷ Thus, the sticky ends not only bias the nanometronome toward *IsoII* but also raise the apparent FRET efficiency of the high FRET state from 0.65 to 0.85 (Figure 2C). If the FRET increase is due to distance decrease, this would indicate that the Holliday junction is relatively flexible and a range of interhelical angles may be allowed within each stacked conformation. It is likely that the length of the overhangs will influence the FRET values of the nanometronome when the sticky end has been base paired.

Figure 4 shows that we can observe the sudden change in the ticking rate of a single nanometronome when the deactivator or the activator strands are added. Here the deactivation/reactivation of the sticky end is monitored in real time using a flow delivery system. In Figure 4A, the time trace starts with a nanometronome having an active five

bp sticky end. At approximately $t = 30$ s, a high concentration ($\sim 1 \mu\text{M}$) of the deactivator is introduced over the immobilized nanometronomes. A sudden transition is clearly seen drastically changing the high FRET dwell time of the nanometronome. Furthermore, E value of the high FRET state drops down from ~ 0.8 to ~ 0.6 , which agrees with results shown in Figure 2C. Figure 4B shows the reverse process where we start the time trace with a silenced nanometronome and flow in the activator strands at approximately $t = 30$ s. Even though the activator strand contains a 5 nt region complementary to the overhang of strand X (see Figure S1 in Supporting Information), a transient “intermolecular” interaction between them does not seem to affect the “intramolecular” sticky end interactions significantly. Figure S2 (Supporting Information) show more examples of these switching events. The whole process is consistently repeatable for several cycles hinting that the removal of the deactivator is complete and our nanometronome can be reset over and over (data not shown).

Our nanometronome can be further controlled to have different lifetimes in the low FRET state (*IsoI*). For example, instead of having just one pair of single-stranded overhangs altering only the high FRET state dwell time, an additional single-stranded overhang can be added to the end of helix X so that base pairing between the overhangs on the helix X and helix B can be used to stabilize the low FRET state (Figure 5A). A representative time trace shows that this version of nanometronome shows increased dwell times for both high and low FRET states.

We have demonstrated that a tunable nanomechanical device, called the nanometronome, can be constructed out of four single-stranded DNA molecules. Our nanometronome is induced to tick by the ambient thermal energy, and the rate of ticking is controlled either by the Mg^{2+} or by

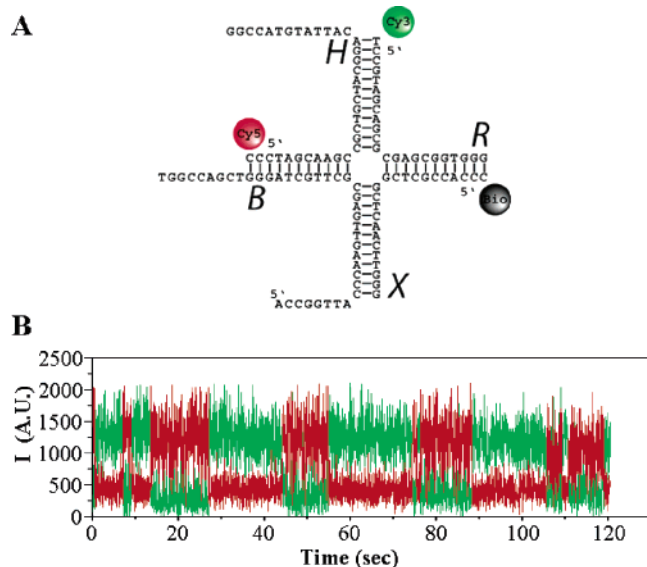


Figure 5. Further modification of nanometronome. (A) Addition of a third single-stranded overhang at the end of helix X could shift the bias of the dwell time toward structure **1**. (B) A sample trace confirms the possibility.

additional controlling elements, single-stranded deactivator and activator. To our knowledge, this is the first demonstration of a DNA-based nanodevice observed at the single molecule level. We learned that even a single base pair difference in the sticky end can be easily detected and single molecular heterogeneity is small enough that even at the single nanometronome level it should be possible to distinguish one base pair difference. Possible applications in the distant future may include the ultrasensitive detection of single nucleotide polymorphism.

Acknowledgment. We thank Adam Dally for experimental help and Robert Clegg for useful discussions. Funding was provided by an NSF CAREER Award and a grant from the National Institutes of Health (GM065367) to T.H. C.B. is a recipient of The Development and Promotion of Science and Technology Talents Project (DPST) Scholarship, Thailand, and S.A.M. is an NSF Graduate Research Fellow.

Supporting Information Available: Descriptions of instrument setup and sample preparation and figures showing sequence information for the nanometronome and additional

sample traces from the flow experiment. This material is available free of charge via the Internet at <http://pubs.acs.org>.

References

- (1) Yurke, B.; Turberfield, A. J.; Mills, A. P.; Simmel, F. C.; Neumann, J. L. A DNA-fuelled molecular machine made of DNA. *Nature* **2000**, *406*, 605–608.
- (2) Li, J. J.; Tan, W. A Single DNA Molecule Nanomotor. *Nano Lett.* **2002**, *2* (4), 315–318.
- (3) Chen, Y.; Wang, M.; Mao, C. An Autonomous DNA Nanomotor Powered by a DNA Enzyme. *Angew. Chem., Int. Ed.* **2004**, *43*, 3554–3557.
- (4) Dittmer, W. U.; Simmel, F. C. Transcriptional Control of DNA-Based Nanomachines. *Nano Lett.* **2004**, *4* (4), 689–691.
- (5) Alberti, P.; Mergny, J.-L. DNA duplex-quadruplex exchange as the basis for a nanomolecular machine. *Proc. Natl. Acad. Sci. U.S.A.* **2003**, *100* (4), 1569–1573.
- (6) Mao, C.; Sun, W.; Shen, Z.; Seeman, N. C. A nanomechanical device based on the B–Z transition of DNA. *Nature* **1999**, *397*, 144–146.
- (7) Liu, D.; Balasubramanian, S. A Proton-Fuelled DNA Nanomachine. *Angew. Chem., Int. Ed.* **2003**, *42*, 5734–5736.
- (8) Liedl, T.; Simmel, F. C. Switching the Conformation of a DNA Molecule with a Chemical Oscillator. *Nano Lett.* **2005**, *5* (10), 1894–1898.
- (9) Viasnoff, V.; Meller, A.; Isambert, H. DNA Nanomechanical Switches under Folding Kinetics Control. *Nano Lett.* **2006**, *6*, 101–104.
- (10) Yan, H.; Zhang, X.; Shen, Z.; Seeman, N. C. A Robust DNA mechanical device controlled by hybridization topology. *Nature* **2002**, *415*, 62–65.
- (11) Feng, L.; Park, S. H.; Reif, J. H.; Yan, H. A Two-State DNA Lattice Switched by DNA Nanoactuator. *Angew. Chem., Int. Ed.* **2003**, *42*, 4342–4346.
- (12) Tyagi, S.; Kramer, F. R. Molecular Beacons: Probes that Fluoresce upon Hybridization. *Nature Biotechnol.* **1996**, *14*, 303.
- (13) Bonnet, G.; Krichevsky, O.; Libchaber, A. Kinetics of conformational fluctuations in DNA hairpin-loops. *Proc. Natl. Acad. Sci. U.S.A.* **1998**, *95*, 8602–8606.
- (14) Holliday, R. A mechanism for gene conversion in fungi. *Genet. Res.* **1964**, *5*, 282–304.
- (15) Lilley, D. M. J., Structures of helical junctions in nucleic acids. *Q. Rev. Biophys.* **2000**, *33* (2), 109–159.
- (16) Duckett, D. R.; Murchie, A. I. H.; Diekmann, S.; Kitzing, E. v.; Kemper, B.; Lilley, D. M. J. The Structure of the Holliday Junction, and Its Resolution. *Cell* **1988**, *55*, 79–89.
- (17) McKinney, S. A.; Déclais, A.-C.; Lilley, D. M. J.; Ha, T. Structural dynamics of individual Holliday junctions. *Nat. Struct. Biol.* **2003**, *10* (2), 93–97.
- (18) Joo, C.; McKinney, S. A.; Lilley, D. M. J.; Ha, T. Exploring Rare Conformational Species and Ionic Effects in DNA Holliday Junctions Using Single-molecule spectroscopy. *J. Mol. Biol.* **2004**, *341*, 739–751.
- (19) Grainger, R. J.; Murchie, A. I. H.; Lilley, D. M. J. Exchange between Stacking Conformers in a Four-Way DNA Junction. *Biochemistry* **1998**, *37*, 23–32.
- (20) Clegg, R. M., Fluorescence resonance energy transfer. *Methods Enzymol.* **1992**, *211*, 353–388.
- (21) Simmel, F. C.; Yurke, B. A DNA-based molecular device switchable between three distinct mechanical states. *Appl. Phys. Lett.* **2002**, *80*, 883–885.

NL052492P

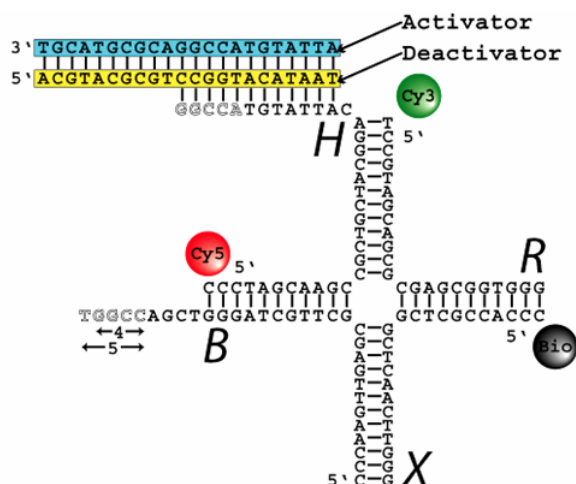
Supporting Information Available

Instrument setup

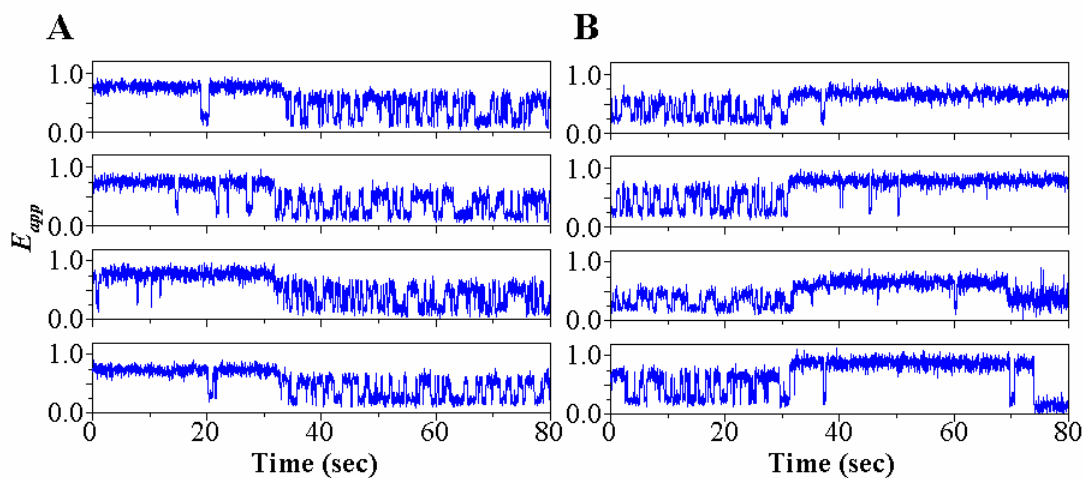
A prism-type total internal reflection (TIR) microscope is used for our single molecule experiment. An inverted microscope (Olympus IX70, Olympus) is equipped with a frequency-doubled Nd-YAG 532 nm laser (Crystalaser) as the excitation source. The excitation beam is focused into a small pellin broca prism (CVI laser) placed on top of the quartz slide with a small drop of immersion oil in between to match the index of refraction. The emitted fluorescence is collected with a high NA water immersion objective (UPLAPO60XW, Olympus). A 550 nm long-pass fluorescence filter (E550LP, Chroma Technology) is used to block the excitation light before passing the fluorescence signal through the side port of the camera. A dichroic mirror with a transmission range of 550-630 nm (645DCXR, Chroma Technology) is used to separate fluorescence signal into two beams: a green channel (550-630 nm) and a red channel (645 nm and above). Finally, two emission beams are focused onto the back of the electron-multiplying CCD camera (IXOR 887-FI, Andor Technology). Data acquisition is handled by the Single software by Sean McKinney (written in Visual C++, Microsoft), and data analysis is performed by either incorporating a traditional edge detection algorithm into a Matlab script (Mathworks) or applying the Viterbi Algorithm (based on Hidden Markov Chain Model) suggested by Sean McKinney.

Sample preparation

Four single-stranded DNA with different sequences and modifications (strand B: 5'-Cy5-CCCTAGCAAGCCGCTGCTACGGACATTATGTACCGG-3'; strand H: 5'-Cy3-TCCGTAGCAGCGCGAGCGGTGGG-3'; strand R: 5'-Biotin-CCCACCGCTCGGCTCAACTTGGG-3'; strand X: 5'-CCCAAGTTGAGCGCTTGCTAGGGTCGA-3') including the deactivator (5'-ACGTACGCGTCCGGTACATAAT-3') and the activator (5'-ATTATGTACCGGACGCGTACGT-3') are purchased from IDT DNA (Integrated DNA Technology Inc.). For four bp and five bp sticky ends (numbered arrows, Figure 1A, *structure 2*), the following sequences are concatenated to the 3' of strand X: CCGG and CCGGT, respectively. All of the ssDNA are PAGE-purified prior to annealing. The annealing process is performed by mixing strand X:B:H:R with the concentration ratio of 2:2:1:1, heating the solution up to 90 C and letting it cool down overnight. After the annealing process, no further purification is made. Prior to single molecule experiments, the integrity of the junction is verified by ensemble FRET measurement. Then, sample immobilization for single molecule experiment is done by applying approximately 100 pM of the complete junction to the quartz surface by a BSA-biotin-neutravidin complex. All measurements are performed at room temperature in 10 mM Tris (pH 8.0), 50 mM NaCl and 50 mM MgCl₂ (except for results in Figure 3) plus oxygen scavenger system.



Supplement Figure S1



Supplement Figure S2

Supplement Figure S1 The sequence information of the nano-metronome including the deactivator (yellow) and the activator (light blue) strands. The design is based on Junction 7 used in the previous work¹⁷ with the addition of a short single stranded overhang, each composed of a spacer region and a sticky region at the end of helix X and at the end of helix B. The arrows represent the position of the sticky ends with numbers corresponding to the number of sticky bases. A solid line links a given pair of

complementary bases. The numbers of bases in the sticky region are chosen based on a requirement that the sticky ends are stable enough to bias the high FRET dwell time but not so strong that very few transitions occurs during the acquisition period. From our preliminary experiments, four and five bases sticky ends are the most suitable. The deactivator (yellow) has a twelve-base complementary to the overhang region of strand B and the other ten nucleotides exposed to the solution. The activator (light blue) is fully complementary to the deactivator.

Supplement Figure S2 Additional sample traces from the flow experiment (from Figure 4). (A) Traces start with active nano-metronomes and at $t \approx 30$ sec the deactivator is added. (B) Traces start with silenced nano-metronomes at at $t \approx 30$ sec the activator is added. The presence of the activator does not significantly alter the function of the sticky ends since the average high and low FRET dwell times are reproducible after the introduction of the activator (data not shown). Even though the activator contains the complementary sequence to the sticky bases of strand X and might potentially act as another deactivator, we believe that the interaction between the activator and the overhang region of strand X (four or five basepairs, depending on the length of the sticky ends) is much weaker than that of the deactivator and the overhang region of strand B (twelve basepairs).